



Cite this: *Dalton Trans.*, 2016, **45**, 9285

## Enantiopure and racemic radical-cation salts of $B(\text{malate})_2^-$ anions with BEDT-TTF $^{\dagger}$

Jordan R. Lopez,<sup>a</sup> Lee Martin,<sup>\*a</sup> John D. Wallis,<sup>a</sup> Hiroki Akutsu,<sup>b</sup> Yasuhiro Nakazawa,<sup>b</sup> Jun-ichi Yamada,<sup>c</sup> Tomofumi Kadoya,<sup>c</sup> Simon J. Coles<sup>d</sup> and Claire Wilson<sup>d</sup>

We have synthesized the first examples of radical-cation salts of BEDT-TTF with chiral borate anions,  $[B(\text{malate})_2]^-$ , prepared from either enantiopure or racemic bidentate malate ligands. In the former case only one of two diastereoisomers of the borate anion is incorporated, while for the hydrated racemic salt one racemic pair of borate anions containing a *R* and a *S* malate ligand is incorporated. Their conducting and magnetic properties are reported. The tight-binding band calculation indicates that the chiral salt has an effective half-filled flat band, which is likely to be caused by the chiral structural feature.

Received 16th March 2016,  
Accepted 10th May 2016

DOI: 10.1039/c6dt01038e

www.rsc.org/dalton

## Introduction

Bis(ethylenedithio)tetrathiafulvene (BEDT-TTF) radical-cation salts have been studied extensively following the discovery of a large number of organic metals and superconductors. These salts have the ability to combine more than one physical property *via* crystal engineering of the conducting BEDT-TTF layers and the insulating anion layers.<sup>1</sup> The synthesis of radical-cation salts of this type offers a promising approach to producing crystalline materials which combine the properties of chirality and conductivity.<sup>2</sup> Electrical magneto-chiral anisotropy was first observed in bismuth helices,<sup>3</sup> and it has also been observed in carbon nanotubes,<sup>4</sup> where the resistivity along nanotubes of opposing chirality differs in a coaxial magnetic field. Pop *et al.* have recently synthesised enantiopure radical-cation salts of (*S,S*)- and (*R,R*)-(DM-EDT-TTF)<sub>2</sub>ClO<sub>4</sub>.<sup>5</sup> These salts, in space groups P6<sub>2</sub>22 and P6<sub>4</sub>22, show metallic behavior down to 40 K and the observation of electrical magneto-chiral anisotropy confirms the chiral nature of charge

transport. The DM-EDT-TTF donor has also produced PF<sub>6</sub> racemic salts with metal-like conductivity, while the enantiopure salts have a completely different packing and show room temperature charge ordering and semiconducting behaviour.<sup>5</sup>

There are three routes through which chirality can be introduced into radical-cation salts: a chiral donor molecule, chiral anion, or a chiral electrolyte. There have been a large number of enantiopure TTF-based donor molecules synthesised since the first example, tetramethyl-(*S,S,S,S*)-BEDT-TTF, in 1986.<sup>6</sup> Recent promise of the use of chiral donor molecules to produce bulk chiral conductors is evidenced by the aforementioned work of Pop *et al.*<sup>5</sup> Recently a semiconducting TTF-type donor has shown lower activation energy for its racemic salt with BF<sub>4</sub> compared to the isostructural analogues for both individual enantiomers.<sup>7</sup>

Other examples of salts from chiral donor molecules include hydroxyalkyl-BEDT-TTFs,<sup>8</sup> bis(oxazoline)-TTFs,<sup>9</sup> iodo-TTFs,<sup>10</sup> pyrrolo-TTFs,<sup>11</sup> and TTF-sulphoxides which have chiral sulphur atoms.<sup>12</sup>

Racemic and chiral anions have been used to produce radical-cation salts with BEDT-TTF including Fe(croconate)<sub>3</sub>,<sup>13</sup> Cr(2,2'-bipy)(oxalate)<sub>2</sub>,<sup>14</sup> Sb<sub>2</sub>(L-tartrate)<sub>2</sub>,<sup>15</sup> TRISPHAT<sup>16</sup> and Fe(C<sub>6</sub>O<sub>4</sub>Cl<sub>2</sub>)<sub>3</sub>.<sup>17a</sup> Fe(C<sub>6</sub>O<sub>4</sub>Cl<sub>2</sub>)<sub>3</sub> has also been combined in salts with TM-BEDT-TTF<sup>17b</sup> in a rare case where a chiral donor and chiral anion have been combined, although the anion crystallised as a racemic mixture. An enantiopure bis-hydroxy-substituted TTF donor has also produced a 4 : 1 salt with the *meso* stereoisomer of the dinuclear [Fe<sub>2</sub>(oxalate)<sub>5</sub>]<sup>4-</sup> anion.<sup>8</sup>

The most extensive family of BEDT-TTF salts with chiral anions contain tris(oxalato)metallate and these have provided a large number of materials which combine magnetism with

<sup>a</sup>School of Science and Technology, Nottingham Trent University, Clifton Lane, Clifton, Nottingham, NG11 8NS, UK. E-mail: lee.martin@ntu.ac.uk; Tel: +44 (0)1158483128

<sup>b</sup>Department of Chemistry, Graduate School of Science, Osaka University, 1-1 Machikaneyama-cho, Toyonaka, Osaka 560-0043, Japan

<sup>c</sup>Graduate School of Material Science, University of Hyogo, Kamigori-cho, Ako-gun, Hyogo 678-1297, Japan

<sup>d</sup>School of Chemistry, Faculty of Natural and Environmental Sciences, University of Southampton, Highfield, Southampton, SO17 1BJ, UK

<sup>†</sup>Electronic supplementary information (ESI) available. CCDC 1468076–1468078. For ESI and crystallographic data in CIF or other electronic format see DOI: 10.1039/c6dt01038e



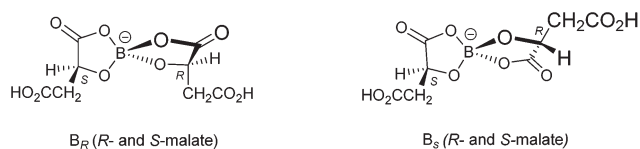
conductivity in the same lattice.<sup>18</sup> These salts contain a 50 : 50 mixture of the  $\Delta$  and  $\Lambda$  enantiomers of  $[M^{III}(\text{oxalate})_3]^{3-}$  to give an overall racemic lattice.<sup>19</sup> However, the spatial distribution of these two enantiomers within the anion layers determines the donor packing arrangement and thus the conducting properties.

The inclusion of a guest solvent molecule within the lattice of these tris(oxalato)metallate salts introduces the possibility of using a chiral solvent for crystal growth. Crystals containing either enantiopure or racemic *sec*-phenethyl alcohol molecules show a difference in their conducting properties owing to the disorder of the enantiomers of the guest solvent molecule in the anion layer of the racemic salt.<sup>20</sup> Recently, the first examples containing a single enantiomer of tris(oxalato)metallate in the lattice have been produced by using chiral induction through electrocrystallisation from the chiral electrolyte (*R*)-carvone containing racemic  $\text{Cr}(\text{C}_2\text{O}_4)_3$  or  $\text{Al}(\text{C}_2\text{O}_4)_3$ .<sup>21</sup>

We report here two new BEDT-TTF radical-cation salts incorporating the anion  $\text{B}(\text{malate})_2^-$  prepared from either racemic malic acid or enantiopure *D*-(+)-malic acid. The synthesis of such bis-chelated borate anions offers the prospect of creating complexes with more than one stereogenic centre. In the case of the  $\text{B}(\text{malate})_2^-$  reported here the chirality of the bidentate chelated malate ligand is retained but diastereomers are produced through two possible stereochemical configurations at the boron centre which is labile in solution. Therefore, when using enantiopure *D*-(+)-malic acid ((*R*)-hydroxybutanedioic acid), a mixture of diastereoisomeric anions will be produced:  $\text{B}_S\text{RR}$  with an *S* boron centre and two *R* malate ligands, and  $\text{B}_R\text{RR}$  which differs only in having an *R* boron centre (Scheme 1). <sup>1</sup>H NMR in deuterio-acetonitrile shows the anions exist in a 2 : 1 ratio with very similar NMR spectra. When using racemic *DL*-malic acid, four further diastereomers will be produced:  $\text{B}_S\text{SS}$  and  $\text{B}_R\text{SS}$  (the mirror images of the anions shown in Scheme 1) and  $\text{B}_S\text{RS}$  and  $\text{B}_R\text{RS}$  (Scheme 2). <sup>1</sup>H NMR in deuterio-acetonitrile is complex but consistent with the presence of these diastereomers.  $\text{B}_S\text{RR}$ ,



**Scheme 1** The two borate anions which can be formed using *D*-(+)-malic acid.



**Scheme 2** The two borate anions containing both malate enantiomers.

$\text{B}_R\text{RR}$  and  $\text{B}_S\text{SS}$ ,  $\text{B}_R\text{SS}$  are racemic pairs and therefore only four signals are expected.

We report here a chiral radical-cation salt of BEDT-TTF, synthesised electrochemically in the presence of chiral  $\text{B}_S\text{RR}$  and  $\text{B}_R\text{RR}$  anions, in which just the  $\text{B}_S\text{RR}$  anion is incorporated into the structure. When repeating this synthesis using a mixture of the six possible diastereomeric borate anions prepared from racemic malic acid a racemic radical-cation salt is obtained but only two of the diastereomeric anions are present in the crystal ( $\text{B}_S\text{RS}$  and  $\text{B}_R\text{RS}$ ).

## Results and discussion

### $(\text{BEDT-TTF})_2\text{B}_{R/S}[(R/S)\text{-malate}]_2(\text{H}_2\text{O})_{2.85}$ (**I**)

Radical-cation salt **I** was synthesised by electrocrystallisation of BEDT-TTF in 1,1,2-trichloroethane containing 18-crown-6 and the mixture of potassium borate salts prepared from racemic malic acid. Salt **I** has the formula  $(\text{BEDT-TTF})_2\text{B}_{R/S}[(R/S)\text{-malate}]_2(\text{H}_2\text{O})_{2.85}$  with only two of the possible diastereomers present in the radical-cation salt. Salt **I** crystallises in the triclinic crystal system in the centrosymmetric space group  $P\bar{1}$ . The asymmetric unit consists of two crystallographically independent BEDT-TTF molecules, one borate anion and 2.85 water molecules (Fig. 1). The borate anion contains one *R*- and one *S*-malate anion. The unit cell thus contains a racemic pair of two such anions, differing only in the configuration at boron (*R* or *S*) (Fig. 2). This is the first example of diastereomeric induction within the electrocrystallisation environment without the need for external auxiliaries. Previously chiral radical-cation salts have been synthesised from enantiopure

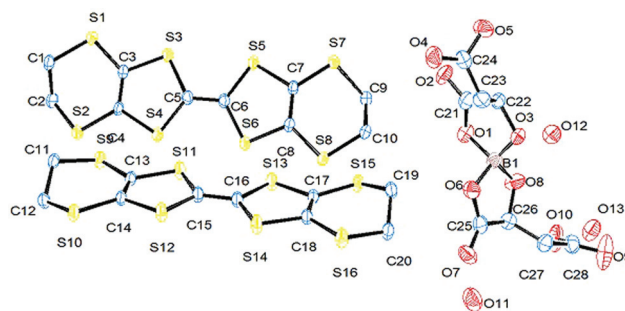


**Fig. 1** ORTEP diagram of the asymmetric unit of **I** showing atomic labelling, hydrogens are omitted for clarity.

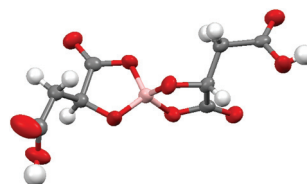


**Fig. 2** Borate anion in **I**.



anions,<sup>15,16</sup> or from racemates which have been resolved during crystal engineering in chiral solvents.<sup>21</sup> The two independent donors are separately stacked along the *a* axis. The stacks lie side by side in the *b* direction to form a layer and with an angle of 70.64° between the best planes of the independent donors. This corresponds to the  $\alpha$ -type packing arrangement of BEDT-TTF donors. Donor layers are separated by layers containing the borate anions and hydrogen bonded water molecules (Fig. 3). The anion layer contains 2.85 waters per borate anion. The two carboxylic hydrogen atoms are hydrogen bonded to water molecules (1.78–1.85 Å), one of the waters is also hydrogen bonded to two borate ring O atoms (2.05 and 2.15 Å), while the other water is also hydrogen bonded to a ring carbonyl oxygen (2.20 Å) and to a third water molecule (1.99 Å). This third water molecule makes a second hydrogen bond to a ring carbonyl O atom (1.93 Å) (Fig. 4).

The terminal ethylene carbons of each donor show half chair conformations with each sp<sup>3</sup> carbon equidistant from the plane of the TTF unit. The two donors each have thirteen side-to-side S...S contacts below the sum of van der Waals

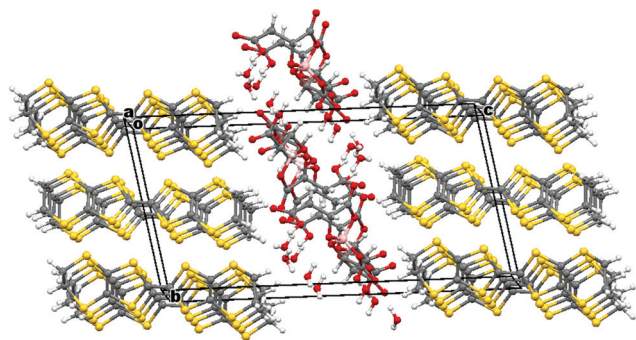


Fig. 3 Layered structure of I viewed down the *a* axis.

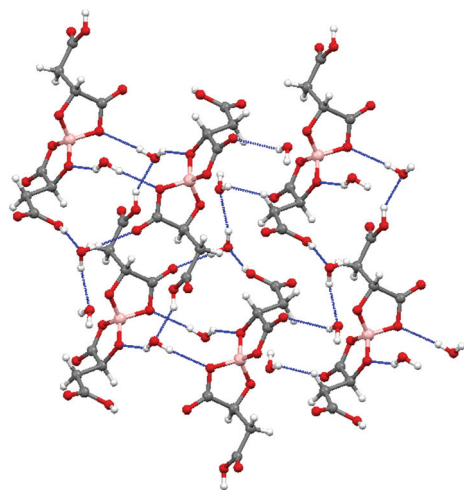


Fig. 4 Anion layer of I.

Table 1 S...S contacts shorter than the van der Waals distance for I

S...S	Donor A...B Contact/Å
S1...S10	3.53(1)
S1...S12	3.58(1)
S5...S16	3.47(1)
S7...S16	3.58(1)
S2...S9	3.48(1)
S4...S9	3.56(1)
S8...S13	3.55(1)
S8...S15	3.49(1)
S8...S10	3.48(1)
S8...S12	3.57(1)
S1...S13	3.47(1)
S1...S15	3.46(1)
S7...S9	3.56(1)

radii (Table 1). These contacts are all side-to-side between neighbouring stacks of crystallographically independent donors. Donor A has two short contacts with two of the H<sub>2</sub>O molecules (S7–O13, 3.285 Å and S2–O11, 3.142 Å) and donor B has one short contact with a borate anion (S10–O4, 3.145 Å) (Fig. 4).

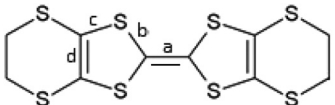
The molecular formula suggests that the two independent donors have a cumulative charge of +1 to balance the charge of the B<sub>R/S</sub>[(*R/S*)-malate]<sub>2</sub><sup>−</sup> anion. Using the method of Guionneau *et al.*<sup>22</sup> for estimating oxidation state from molecular geometry the two donors are calculated each to carry a charge of 0.5<sup>+</sup> (Table 2). The central C=C bond lengths are 1.366 Å in both A and B donors.

The resistivity of I shows exponential temperature dependence only below ~250 K with an activation energy of 0.050 eV ( $\rho_{RT} = 0.00163 \Omega \text{ cm}$ ) (Fig. 5).

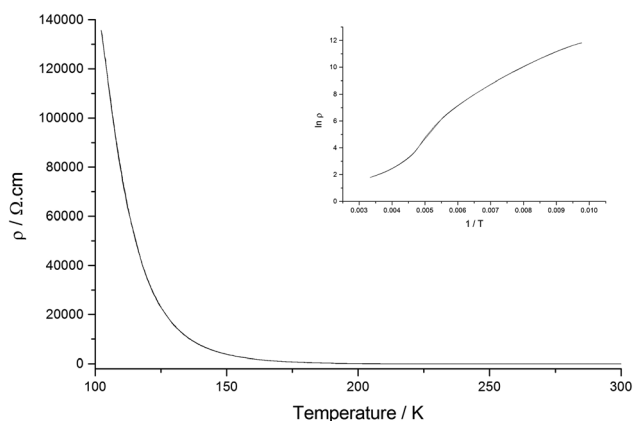
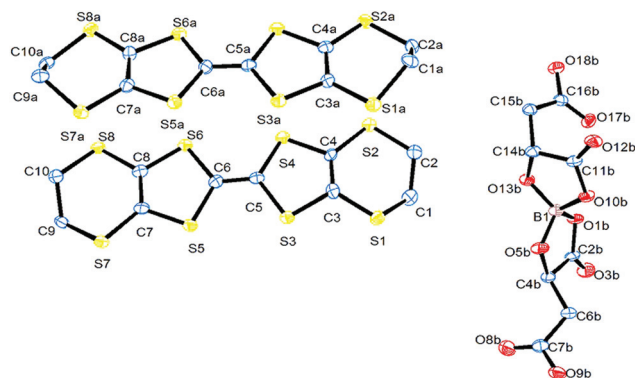
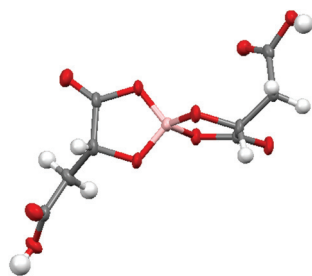
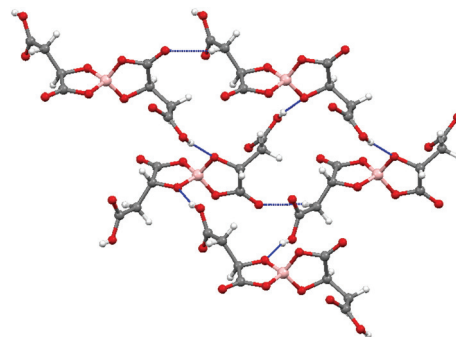
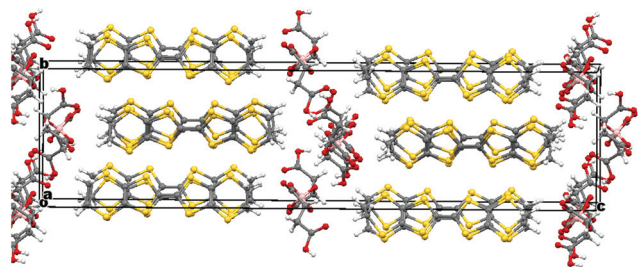
#### (BEDT-TTF)<sub>2</sub>[B<sub>S</sub>(*R*-malate)<sub>2</sub>] (II)

The electrochemical synthesis using the [B<sub>R/S</sub>(*R*-malate)<sub>2</sub>] anion mixture prepared from enantiopure D-(+)-malic acid does not give an isostructural radical-cation salt. Instead, salt II with formula (BEDT-TTF)<sub>2</sub>[B<sub>S</sub>(*R*-malate)<sub>2</sub>] is synthesized which contains only the borate anion with stereochemistry B<sub>S</sub>RR and no water (Fig. 6). Salt II crystallises in the orthorhombic crystal system in the space group *P*2<sub>1</sub>2<sub>1</sub>2<sub>1</sub>. The crystal packing is shown in Fig. 7. Two crystallographically independent donors and one borate anion are present in the asymmetric unit (Fig. 8). The two independent donors are organised in an ABAB arrangement in stacks along the *a* axis, with the adjacent donors lying at an angle of 10°. The stacks lie side by side in an  $\alpha$  packing arrangement to form layers perpendicular to the *c* axis. Adjacent layers are separated by layers composed of the chiral borate anions. The anions form layers held together by hydrogen bonding between the carboxylic acid groups and borate ring O atoms (Fig. 9). The CH<sub>2</sub>CO<sub>2</sub>H side chains adopt different conformations, one extended away from the borate and the other folded back so the acid's carbonyl oxygen makes a short contact with the adjacent ring carbonyl carbon (O...C: 2.738 Å). There is also a short



**Table 2** Average bond lengths and estimation of charge on the BEDT-TTF molecules of I and II.  $\delta = (b + c) - (a + d)$ ,  $Q = 6.347 - 7.463\delta$ .<sup>21</sup>


Salt	Donor	a/Å	b/Å	c/Å	d/Å	$\delta$	Q	Charge
I at 150 K	A	1.366	1.743	1.750	1.358	0.769	0.60+	1.19 ± 0.2 = 1
	B	1.366	1.742	1.752	1.354	0.771	0.59+	
I at 250 K	A	1.366	1.740	1.7525	1.3495	0.777	0.55+	1.13 ± 0.2 = 1
	B	1.366	1.742	1.7505	1.3535	0.773	0.58+	
II	A	1.357	1.762	1.756	1.357	0.804	0.37+	1.31 ± 0.3 = 1
	B	1.379	1.731	1.746	1.373	0.725	0.94+	

**Fig. 5** Resistivity data for I.**Fig. 8** ORTEP diagram of the asymmetric unit of II showing atomic labelling, hydrogens are omitted for clarity.**Fig. 6** Borate anion in II.**Fig. 9** Anion layer of II.**Fig. 7** Layered structure of II viewed down the *b* axis, hydrogens are omitted for clarity.

intermolecular contact from a methylene hydrogen belonging to the extended side chain to a ring carbonyl oxygen (2.37 Å) (Fig. 9). Terminal BEDT-TTF ethylene groups have half chair conformations with  $sp^3$  carbons equidistant from the planar TTF core. There is a network of side-to-side S...S contacts between donors in neighbouring stacks (Table 3). A short contact is observed between donor B and a borate anion (S2A...O17B, 3.043 Å).

The formula  $(\text{BEDT-TTF})_2[\text{B}_5(\text{R-malate})_2]$  suggests that the donors have a cumulative charge of +1 to balance



Table 3 S...S contacts shorter than the van der Waals distance for II

	Donor A...B Contact/Å
S4...S7A	3.48(1)
S8...S1A	3.34(1)
S8...S3A	3.44(1)
S7...S2A	3.45(1)
S7...S4A	3.49(1)
	Donor A...A Contact/Å
S2...S7	3.45(1)
S4...S7	3.48(1)
S3...S8	3.57(1)
	Donor B...B Contact/Å
S8A...S3A	3.54(8)

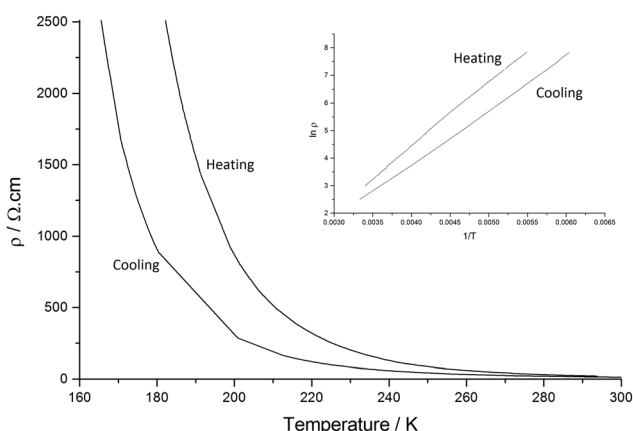


Fig. 10 Resistivity data for II.

the charge of the borate anion. Using the method of Guionneau *et al.*<sup>22</sup> the two crystallographically independent donors carry charges of  $0.94^+$  and  $0.37^+$ , and central C=C bond lengths are 1.357 and 1.379 Å. This indicates charge localisation with a 1+ charge on one donor and the other donor being neutral.

Salt II shows low resistivity at room temperature ( $\rho_{RT} = 15.015 \Omega \text{ cm}$ ) and semiconducting behaviour is observed upon cooling from 300 K to 165 K. Hysteresis is also present on heating back up to 300 K giving a less efficient conductor as we observe an increase in  $E_a$  ( $E_a$  cooling = 0.082 eV,  $E_a$  heating 0.099 eV) (Fig. 10).

### Comparison of salts I and II

As mentioned above, both salts have similar  $\alpha$ -type packing motif and the resistivity behaviours are also similar apart from the anomaly at approximately 190 K on the resistivity curve of I. However, the charge of BEDT-TTF molecules shown in Table 2 indicates that both electronic structures are different,

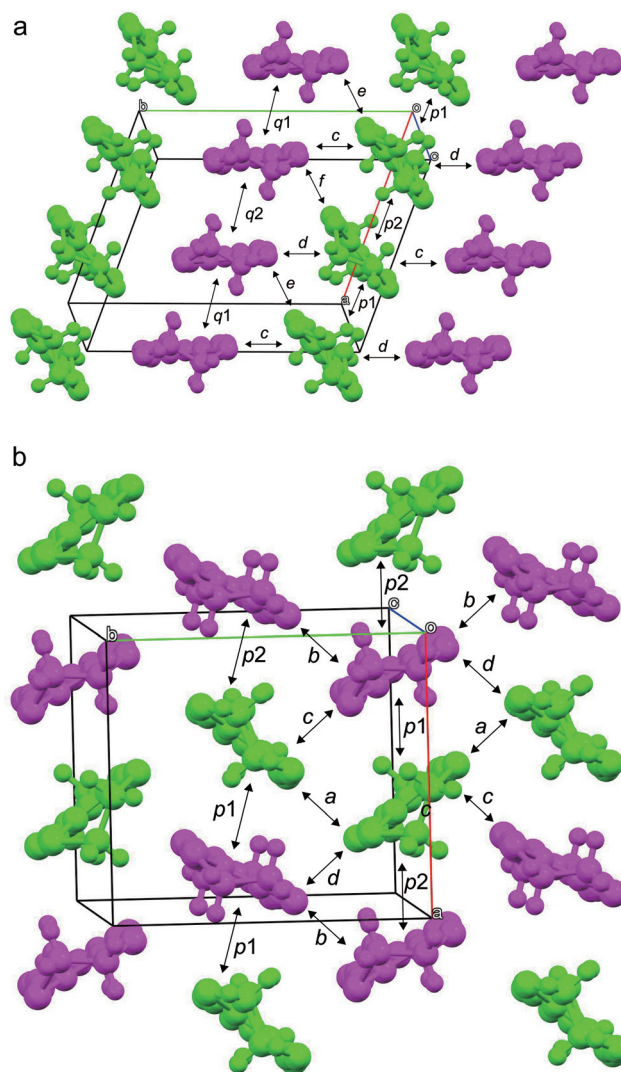
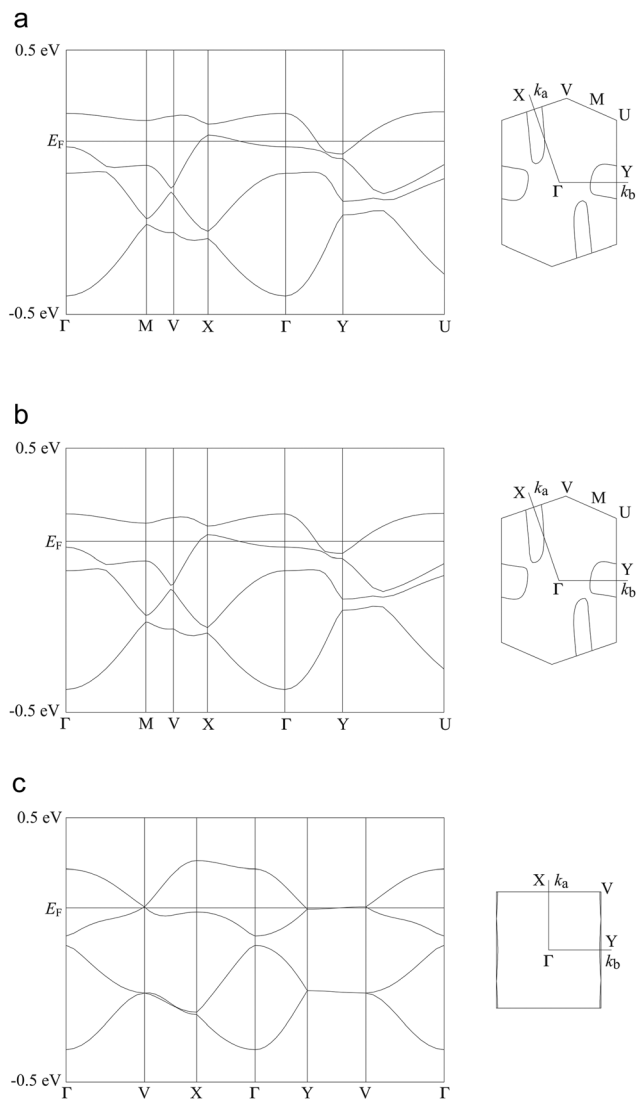


Fig. 11 End of the donor layers of I (a) and II (b). Green and pink coloured molecules are molecules A and B, respectively.

with salt I being metallic at room temperature and salt II in the charge-ordered state at least at 100 K. Therefore, the two salts should have some structural difference. Fig. 11 shows an end-on projection of the donor layers of both salts (I and II), where green and pink coloured molecules are the molecules A and B, respectively. In salt I (Fig. 11a) each crystallographically independent molecule forms a stack along the  $a$  axis. On the other hand, salt II (Fig. 11b) has alternating A and B molecules within each stack. We performed a tight binding band calculation of each of the salts.<sup>23</sup> The calculation neglected the electron correlation effects so that the band calculations provided Fermi surfaces for many quarter-filled salts although the salts are actually semiconductive. In other words, a semiconducting salt possessing Fermi surfaces on the band calculation indicates that the band gap is caused by the electron correlations. The band dispersions and Fermi surfaces of I at 150 and 250 K are shown in Fig. 12a and b, respectively. There is no





**Fig. 12** Band dispersions and Fermi surfaces of salts I (a: 150 K; b: 250 K) and II (c). Transfer integrals ( $\times 10^{-3}$  eV, see also Fig. 11) are  $p1 = -3.07$ ,  $p2 = -7.13$ ,  $q1 = -5.04$ ,  $q2 = -1.67$ ,  $c = -7.41$ ,  $d = -12.21$ ,  $e = +8.32$  and  $f = +6.58$  for salt I at 150 K,  $p1 = -3.21$ ,  $p2 = -6.42$ ,  $q1 = -4.62$ ,  $q2 = -1.97$ ,  $c = -7.25$ ,  $d = -11.42$ ,  $e = +7.93$  and  $f = +6.59$  for salt I at 250 K and  $p1 = +5.07$ ,  $p2 = -1.38$ ,  $a = +5.57$ ,  $b = +10.64$ ,  $c = +16.11$  and  $d = +1.10$  for salt II.

significant difference between the structures of **I** at 150 and 250 K. The band calculation results also have no significant difference between those at 150 and 250 K. Salt **I** has an electron and a hole pocket, which is similar to  $\beta''$ -type salts,<sup>24</sup> and suggests that salt **I** is semi-metallic. Actually the salt is semi-metallic at room temperature. However, at lower temperature, especially below the transition temperature of 190 K, the resistivity increases with decreasing temperature. Usually a semimetal has no temperature dependence of resistivity. This behaviour indicates that the salt becomes a semiconductor in the low temperature region. The molecular charges shown in Table 2 indicate that the salt is not in the

charge disproportionation state, which is paramagnetic, at least down to 150 K. The salt cannot become a paramagnetic Mott insulator because the band dispersion (Fig. 12a) has no Mott gap (see next paragraph). Therefore, it is not likely that the salt has a paramagnetic ground state. Preliminary magnetic susceptibility measurement using only 0.38 mg of powder sample suggests that the data can be fitted by a Curie–Weiss model, we believe that this shows a Curie tail (Fig. S1†), and no magnetic transition was observed. This result strengthens the hypothesis that the ground state is non-magnetic. We speculate at present that the salt becomes a band insulator in the low temperature region by band nesting. Similarly,  $\beta''$ -(BEDT-TTF)<sub>4</sub>[(H<sub>3</sub>O)Cr(C<sub>2</sub>O<sub>4</sub>)<sub>3</sub>]-CH<sub>2</sub>Cl<sub>2</sub> shows semi-conducting behaviour although the salt has semimetallic Fermi surfaces.<sup>25</sup>

As mentioned above, although salt **II** has a similar  $\alpha$ -type packing motif to salt **I**, the arrangement of the green and pink molecules is different (as shown in Fig. 11b). The band dispersions and Fermi surfaces are shown in Fig. 12c, which is very different to that of salt **I**. The band dispersion has a mid-gap at the centre of the band dispersion, a so-called Mott gap, indicating that the band is effective half filled. So the salt can become a Mott insulator. However, the salt selects a charge-ordered state, in which the charge of the green molecule (A) is almost zero and the charge of the pink molecule (B) is almost one as shown in Table 2. This charge-ordered pattern is the so-called “horizontal stripe”, which is commonly observed in the  $\alpha$ -type BEDT-TTF salts. An  $\alpha$ -type packing motif can theoretically have many types of charge disproportionation states.<sup>26</sup> However, the horizontal stripe type is the most common, which was observed in salt **II**, and a vertical type, which salt **I** may have if the salt becomes a charge-ordered state, is not common. Although, salt **II** has the common horizontal stripe type charge order for  $\alpha$ -type BEDT-TTF salts, the band structure is very different from usual  $\alpha$ -type BEDT-TTF salts. As shown in Fig. 12c, an effectively half-filled flat band is observed from Y to V, on which the Fermi level is located. The resultant Fermi surfaces are straight line like a 1D band located on the edge of the Brillouin zone. The band structure of the usual  $\alpha$ -type BEDT-TTF salts consists of quasi-1D and 2D Fermi surfaces, similar to the  $\kappa$ - or  $\lambda$ -type Fermi surface. The comparison of the transfer integrals indicates that the  $b$  and  $c$  (see Fig. 11b) values are almost twice as large as those of normal  $\alpha$ -type BEDT-TTF salts. This indicates that salt **II** has strong 1D nature along the side-by-side,  $b$ -axis direction. If we change the value of the transfer integrals of  $b$  and  $c$  into the half values, the calculation provides the common  $\alpha$ -type Fermi surfaces. Magnetic susceptibility measurement using 2.70 mg of powder sample of **II** (Fig. 13) suggests that the magnetic curve obeys a 2D Heisenberg model with  $J = -71.1$  K but with a spin concentration of only 25%. A residual temperature independent magnetic susceptibility of  $5.7 \times 10^{-4}$  emu mol<sup>-1</sup> was observed, suggesting that some fraction of the electrons are still itinerant. The strong side-by-side interaction may make some percentage (75%?) of spin freedom. The observation of



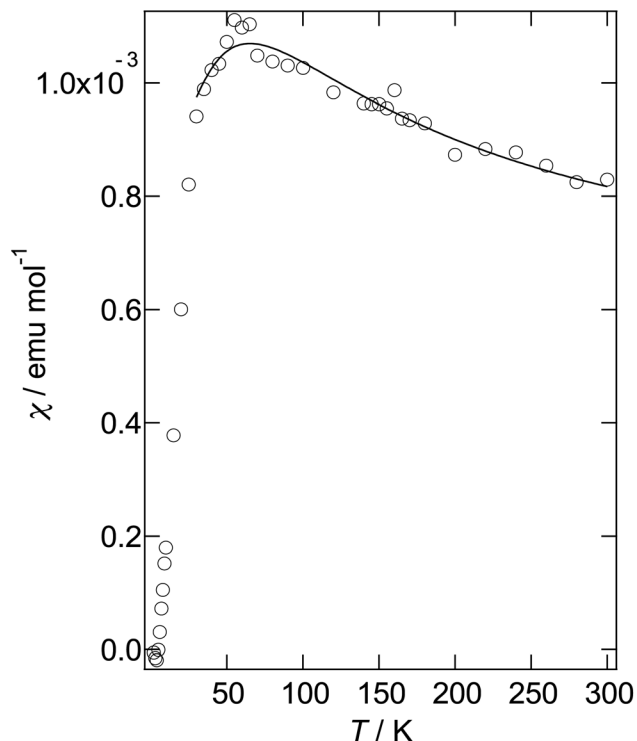


Fig. 13 Magnetic susceptibility of II after subtracting a Curie tail of 0.80% of  $S = 1/2$  spin. The solid line is calculated on the basis of a 2D Heisenberg model.<sup>27</sup>

the separation of the charge and spin freedom may be due to the polar nature of the crystal (see below). In addition, materials having a half-filled flat band can become ferromagnetic, which is so called Flat-Band Ferromagnetism.<sup>28</sup> Salt II may be a candidate for a Flat-Band Ferromagnet. Now the sample has a band gap in the middle of the effective upper band caused by charge ordering. Applying static or uniaxial pressure to the sample can make the band gap become null, and the sample may become a ferromagnet. Moreover, a flat band material may have such a large density of state that it may have a large Seebeck coefficient.<sup>29</sup> It is therefore a candidate for a thermoelectric transducer. Further research is now in progress.

We believe that the unique electronic structure of salt II is owing to its chiral and polar anion. We calculated the dipole moment of the chiral anion using Winmostar Ver.4.104<sup>30</sup> (MOPAC AM1) using atomic coordinates of the crystal structure. A dipole moment of 5.104 Debye is calculated, which directs to approximately the crystallographic  $c$  axis (Fig. S2a†). However, there are two anions in the anion layer, both of which appear to be arranged to cancel both dipole moments. Therefore the calculation of the dipole moment of both anions was performed. A dipole moment of 3.103 Debye was calculated, which was still large. The dipole vector directs to approximately the  $-a$  direction (Fig. S2b†). For the cancellation of the dipole moment along the  $a$  axis, the donor layer appears to go into the 0101 charge-ordered state along the  $a$  axis.

Finally we calculated the dipole moment of four anions that surround a donor layer. A residual dipole moment of 1.431 Debye was calculated, which directs to the  $-b$  direction. The dipole moment can be converted into a voltage using the equation,  $\Delta\Phi = \mu N \cos \theta / \epsilon \epsilon_0$  (ref. 31) = 0.14 eV, where  $\epsilon \approx 2$  and  $\theta = 0.0^\circ$  were assumed.

The dipole moment caused by the anion layer should be cancelled, for which the donor layers should also be polarized. The donor layers would be in a unique charge disproportionate state to produce dipole moments also along the  $b$ -axis. In the circumstance, we speculate that the strong 1D interaction of salt II along the  $b$  axis, which provides the unique flat band, is owing to the residual dipole moment, whose origin is the chirality of the borate anion, because a crystal including a chiral molecule cannot possess any inversion centres or mirror and glide planes and become chiral and polar. Thus we believe that chirality provides a significant effect upon the electronic structure.

## Experimental

### Synthesis and purification of starting materials

BEDT-TTF was purchased from Sigma Aldrich and recrystallised from chloroform. 1,1,2-trichloroethane, L-(–)-malic acid, D-(+)-malic acid, D/L-malic acid, boric acid, sodium hydroxide and 18-crown-6 were purchased from Sigma Aldrich and used as received.

### Synthesis of $\text{K}[\text{B}(\text{malate})_2]^{32}$

Boric acid (2.47 g, 40.0 mmol, 1.00 equiv.) was added to a solution of racemic D/L-malic acid (10.73 g, 80.0 mmol, 2.00 equiv.) in water (10 ml). To this was added a solution of KOH (2.08 g, 40.0 mmol, 1.00 equiv.) in water (30 ml) and the reaction mixture stirred at 95 °C. After evaporation of the water  $\text{K}[\text{B}(\text{malate})_2]$  was isolated as a white powder. The same method was used replacing D/L-malic acid with either L-(–)-malic acid or D-(+)-malic acid. Yields >99% yield in all cases.

Racemic Salt;  $\delta_H$  (400 MHz,  $\text{CD}_3\text{CN}$ ): four diastereomers, 4.44–4.51 (2H, m) ( $2 \times \text{OCH}$ ), 2.65–2.74 (2H, m) ( $2 \times \text{CH}_\alpha\text{H}_\beta\text{CO}_2\text{H}$ ), 2.46–2.55 (2H, m) ( $2 \times \text{CH}_\alpha\text{H}_\beta\text{CO}_2\text{H}$ );  $\delta_C$  (100 MHz,  $\text{CD}_3\text{CN}$ ): 178.3 & 178.4 ( $2 \times \text{CO}_2\text{B}$ ), 171.8 ( $2 \times \text{CO}_2\text{H}$ ), 72.2 & 72.4 ( $2 \times \text{OCH}$ ), 38.87, 38.91, 39.11 & 39.14 ( $2 \times \text{CH}_2\text{CO}_2\text{H}$ ). CHN:  $\text{K}[\text{B}(\text{C}_4\text{O}_5\text{H}_4)_2] \cdot \text{H}_2\text{O}$ ; expected: C 28.95%, H 3.01%; found: C 28.94%, H 3.04%.

Chiral Salt;  $\delta_H$  (400 MHz,  $\text{CD}_3\text{CN}$ ): two diastereomers in ratio 2 : 1, 4.47 (2H, dd,  $J = 7.9, 4.3$  Hz, major) & 4.49 (2H, dd,  $J = 8.6, 4.2$  Hz, minor) ( $2 \times \text{OCH}$ ), 2.67 (2H, dd,  $J = 15.6, 4.2$  Hz, minor) & 2.71 (2H, dd,  $J = 15.8, 4.3$  Hz, major) ( $2 \times \text{CH}_\alpha\text{H}_\beta\text{CO}_2\text{H}$ ), 2.49 (2H, dd,  $J = 15.6, 8.6$  Hz, minor) & 2.52 (2H, dd,  $J = 15.8, 7.9$  Hz, major) ( $2 \times \text{CH}_\alpha\text{H}_\beta\text{CO}_2\text{H}$ );  $\delta_C$  (100 MHz,  $\text{CD}_3\text{CN}$ ): 178.2 & 178.3 ( $2 \times \text{CO}_2\text{B}$ ), 171.8 ( $2 \times \text{CO}_2\text{H}$ ), 72.1 & 72.3 ( $2 \times \text{OCH}$ ), 38.8 & 39.0 ( $2 \times \text{CH}_2\text{CO}_2\text{H}$ ). CHN:  $\text{K}[\text{B}(\text{C}_4\text{O}_5\text{H}_4)_2]$ ; expected: C 30.6%, H 2.57%; found: C 30.32%, H 2.72%.



## Synthesis of radical-cation salts

Crystals of **I** and **II**† were grown on platinum electrodes by electrocrystallisation in 40 ml H-shaped electrochemical cells.

Platinum electrodes were cleaned by applying a voltage across the electrodes in 1 M H<sub>2</sub>SO<sub>4</sub> in each direction to produce H<sub>2</sub> and O<sub>2</sub> at the electrodes, then washed with distilled water and thoroughly dried. K[B(malate)<sub>2</sub>] (100 mg) and 18-crown-6 (200 mg) were dissolved in 1,1,2-trichloroethane (30 ml) with stirring overnight before filtering into an H-cell containing BEDT-TTF (10 mg) in the anode compartment. Salt **I** was prepared using K[B(malate)<sub>2</sub>] synthesized from racemic malic acid. Salt **II** was prepared using K[B(malate)<sub>2</sub>] synthesized from D-(+)-malic acid. H-cells were placed in a dark box on a vibration-free bench at a constant current of 0.2 μA and after 21 days a large number of black hexagonal crystals were harvested from the anode of the H-cell containing the racemic anion. A large number of black plates were collected from the H-cell containing the enantiopure anion. Attempts were also made to grow crystals using K[B(malate)<sub>2</sub>] prepared from L-(−)-malic acid, but despite repeated attempts using a variety of conditions it was not possible to obtain single crystals.

## Physical measurements

Four-probe DC transport measurements were made on crystals using a HUSO HECS 994C multi-channel conductometer. Gold wires (15 μm diameter) were attached to the crystal, and the

attached wires were connected to an integrated circuit plug with carbon conductive cement.

## SQUID magnetometry

Magnetic susceptibility measurements were performed with a Quantum Design MPMS2 SQUID magnetometer using randomly orientated polycrystalline material encased in aluminium foil. Magnetization was recorded from 2 to 300 K at 0.3 and 0.1 Tesla for **I** and **II**.

## Conclusions

Two new radical-cation salts of BEDT-TTF with B(malate)<sub>2</sub><sup>−</sup> have been synthesised. These are the first examples of radical-cation salts of BEDT-TTF with borate anions. The two salts differ by having either chiral or racemic bidentate malate ligands. Both salts have novel packing arrangements of the B(malate)<sub>2</sub><sup>−</sup> diastereomers and show preference for certain diastereomers over others in the electrochemical synthesis. Both salts show α-type BEDT-TTF packing but differ in the distribution of the crystallographically independent donor molecules. The racemic salt has donor stacks which contain only a single crystallographically independent donor molecule and is metallic at room temperature. The chiral salt has donor stacks which contain both donors in alternating ABAB fashion, and this salt is in the charge-ordered state showing semiconducting behaviour.

We have synthesised a variety of borate anions with numerous chiral ligands and are continuing to synthesise further salts with BEDT-TTF to closely examine the effect of chirality upon the physical properties. We are also performing experiments using chiral hydroxylalkyl-BEDT-TTF derivatives with the aim of transmitting the chirality between anion and conducting donor layers through hydrogen-bonding interactions.

## Acknowledgements

This work has been supported by the Royal Society [Research Grants (RG100853 and RG081209), International Exchange Scheme (IE130367), and International Joint Project (JP0869972)]. We thank EPSRC for funding the National Crystallography Service. JRL and LM thank NTU for a PhD studentship.

## Notes and references

- 1 For a series of reviews, see: *Chem. Rev.*, 2004, **104**, passim; *J. Phys. Soc. Jpn.*, 2006, **75**, passim; J. M. Williams, J. R. Ferraro, R. J. Thorn, K. D. Carlson, U. Geiger, H. H. Wang, A. M. Kini and M. H. Whangbo, *Organic Superconductors: Synthesis, Structure, Properties and Theory*, Prentice Hall, Englewood Cliffs, NJ, 1992.
- 2 N. Avarvari and J. D. Wallis, *J. Mater. Chem.*, 2009, **19**, 4061.

† Crystal data: **I** at 150 K: C<sub>28</sub>H<sub>29.44</sub>O<sub>12.72</sub>S<sub>16</sub>B<sub>1</sub>, *M* = 1093.26, black plate, *a* = 8.6620(4), *b* = 11.9323(5), *c* = 21.7062(7) Å, α = 76.855(5), β = 84.526(6), γ = 70.436(5)°, *U* = 2058.16(16) Å<sup>3</sup>, *T* = 150 K, space group *P* $\bar{1}$ , *Z* = 2, μ = 0.901 mm<sup>−1</sup>, reflections collected = 19 802, independent reflections = 15 717, *R*<sub>1</sub> = 0.0450, *wR*<sub>2</sub> = 0.1125 [*F*<sup>2</sup> > 2σ(*F*<sup>2</sup>)], *R*<sub>1</sub> = 0.0623, *wR*<sub>2</sub> = 0.1205 (all data).

Crystal data: **I** at 250 K: C<sub>28</sub>H<sub>29.43</sub>O<sub>12.72</sub>S<sub>16</sub>B<sub>1</sub>, *M* = 1093.25, black plate, *a* = 8.7239(3), *b* = 12.0104(3), *c* = 21.7699(6) Å, α = 76.913(5), β = 84.377(6), γ = 70.239(5)°, *U* = 2090.34(14) Å<sup>3</sup>, *T* = 250 K, space group *P* $\bar{1}$ , *Z* = 2, μ = 0.887 mm<sup>−1</sup>, reflections collected = 20 303, independent reflections = 14 953, *R*<sub>1</sub> = 0.0502, *wR*<sub>2</sub> = 0.1229 [*F*<sup>2</sup> > 2σ(*F*<sup>2</sup>)], *R*<sub>1</sub> = 0.0773, *wR*<sub>2</sub> = 0.1353 (all data). Data was collected on three different crystals of **I** confirming that the same diastereomeric anions were present in each crystal.

Crystal data: **II**: C<sub>28</sub>H<sub>24</sub>O<sub>10</sub>S<sub>16</sub>B<sub>1</sub>, *M* = 1044.24, black plate, *a* = 9.1696(8), *b* = 10.2343(9), *c* = 41.196(4) Å, α = β = γ = 90°, *U* = 3866.0(6) Å<sup>3</sup>, *T* = 100 K, space group *P*2<sub>1</sub>2<sub>1</sub>2<sub>1</sub>, *Z* = 4, μ = 0.950 mm<sup>−1</sup>, reflections collected = 44 369, independent reflections = 8836, Flack Parameter = 0.04(9), *R*<sub>1</sub> = 0.0760, *wR*<sub>2</sub> = 0.1891 [*F*<sup>2</sup> > 2σ(*F*<sup>2</sup>)], *R*<sub>1</sub> = 0.0825, *wR*<sub>2</sub> = 0.1980 (all data). Identical unit cells were collected on four different crystals of **II** from one H-cell and two different crystals of **II** from another H-cell suggesting that the crystals were isostructural in having a single B(malate)<sub>2</sub> diastereomer. The small crystal size prevented collection of further full datasets to confirm if all crystals contained the same B<sub>s</sub>(*R*-malate)<sub>2</sub> or if some instead contained B<sub>s</sub>(*R*-malate)<sub>2</sub>.

Data for **I** were collected on a Rigaku R-Axis VII imaging plate system with FR-E SuperBright High-Brilliance Rotating Anode Generator with confocal monochromated MoKα radiation, using a Rapid Auto software for control and processing.

Data for **II** were collected on a Rigaku AFC12 diffractometer with Mo rotating anode, using standard control and processing software. All structures were solved and refined with programs from the SHELX family of computer programs.

CCDC 1468076–1468078 contains supplementary X-ray crystallographic data for **I** and **II**.





- 3 G. L. J. A. Rikken and E. Raupach, *Nature*, 1997, **390**, 493; G. L. J. A. Rikken, J. Folling and P. Wyder, *Phys. Rev. Lett.*, 2001, **87**, 236602.
- 4 V. Krstic, S. Roth, M. Burghard, K. Kern and G. L. J. A. Rikken, *J. Chem. Phys.*, 2002, **117**, 11315; V. Krstic and G. L. J. A. Rikken, *Chem. Phys. Lett.*, 2002, **364**, 51; G. L. J. A. Rikken, *Science*, 2011, **331**, 864.
- 5 F. Pop, P. Auban-Senzier, E. Canadell, G. L. J. A. Rikken and N. Avarvari, *Nat. Commun.*, 2014, **5**, 3757, DOI: 10.1038/ncomms4757; F. Pop, P. Auban-Senzier, A. Frackowiak, K. Ptaszyński, I. Olejniczak, J. D. Wallis, E. Canadell and N. Avarvari, *J. Am. Chem. Soc.*, 2013, **135**, 17176–17186.
- 6 J. D. Dunitz, A. Karrer and J. D. Wallis, *Helv. Chim. Acta*, 1986, **69**, 69.
- 7 L. Martin, J. D. Wallis, M. A. Guziak, J. Oxspring, J. R. Lopez, S.-i. Nakatsuji, J.-i. Yamada and H. Akutsu, *CrystEngComm*, 2014, **16**, 5424.
- 8 I. Awgheda, S. Krivickas, S. Yang, L. Martin, M. A. Guziak, A. C. Brooks, F. Pelletier, M. Le Kerneau, P. Day, P. Horton, H. Akutsu and J. D. Wallis, *Tetrahedron*, 2013, **69**, 8738; S. J. Krivickas, C. Hashimoto, J. Yoshida, A. Ueda, K. Takahashi, J. D. Wallis and H. Mori, *Beilstein J. Org. Chem.*, 2015, **11**, 1561; F. Leurquin, T. Ozturk, M. Pilkington and J. D. Wallis, *J. Chem. Soc., Perkin Trans. 1*, 1997, 3173–3178.
- 9 F. Riobé and N. Avarvari, *Chem. Commun.*, 2009, 3753.
- 10 J. Lieffrig, R. Le Pennec, O. Jeannin, P. Auban-Senzier and M. Fourmigué, *CrystEngComm*, 2013, **15**, 4408.
- 11 S. Yang, A. C. Brooks, L. Martin, P. Day, H. Li, P. Horton, L. Male and J. D. Wallis, *CrystEngComm*, 2009, **11**, 993.
- 12 M. Chas, M. Lemarié, M. Gulea and N. Avarvari, *Chem. Commun.*, 2008, 220; M. Chas, F. Riobé, R. Sancho, C. Mingullón and N. Avarvari, *Chirality*, 2009, **21**, 818.
- 13 C. J. Gómez-García, E. Coronado, S. Curreli, C. Giménez-Saiz, P. Deplano, M. L. Mercuri, L. Pilia, A. Serpe, C. Faulmann and E. Canadell, *Chem. Commun.*, 2006, 4931.
- 14 A. M. Madalan, E. Canadell, P. Auban-Senzier, D. Brânzea, N. Avarvari and M. Andruh, *New J. Chem.*, 2008, **32**, 333.
- 15 E. Coronado, J. R. Galán-Mascarós, C. J. Gómez-García, A. Murcia-Martinez and E. Canadell, *Inorg. Chem.*, 2004, **43**, 8072.
- 16 M. Clemente-León, E. Coronado, C. J. Gómez-García, A. Soriano-Portillo, S. Constant, R. Frantz and J. Lacour, *Inorg. Chim. Acta*, 2007, **360**, 955; F. Riobé, F. Piron, C. Réthoré, A. M. Madalan, C. J. Gómez-García, J. Lacour, J. D. Wallis and N. Avarvari, *New J. Chem.*, 2011, **35**, 2279–2286.
- 17 (a) S. Benmansour, E. Coronado, C. Giménez-Saiz, C. J. Gómez-García and C. Rößer, *Eur. J. Inorg. Chem.*, 2014, **24**, 3949; (b) M. Atzori, F. Pop, P. Auban-Senzier, C. J. Gómez-García, E. Canadell, F. Artizzu, A. Serpe, P. Deplano, N. Avarvari and M. L. Mercuri, *Inorg. Chem.*, 2014, **53**, 7028; (c) M. Atzori, F. Pop, P. Auban-Senzier, R. Clérac, E. Canadell, M. L. Mercuri and N. Avarvari, *Inorg. Chem.*, 2015, **54**, 3643–3653.
- 18 M. Kurmoo, A. W. Graham, P. Day, S. J. Coles, M. B. Hursthouse, J. L. Caulfield, J. Singleton, F. L. Pratt, W. Hayes, L. Ducasse and P. Guionneau, *J. Am. Chem. Soc.*, 1995, **117**, 12209; L. Martin, S. S. Turner, P. Day, P. Guionneau, J. K. Howard, D. E. Hibbs, M. E. Light, M. B. Hursthouse, M. Uruichi and K. Yakushi, *Inorg. Chem.*, 2001, **40**, 1363; T. G. Prokhorova, S. S. Khasanov, L. V. Zorina, L. I. Buravov, V. A. Tkacheva, A. A. Baskakov, R. B. Morgunov, M. Gener, E. Canadell, R. P. Shibaeva and E. B. Yagubskii, *Adv. Funct. Mater.*, 2003, **13**, 403; E. Coronado, S. Curreli, C. Giménez-Saiz and C. J. Gómez-García, *Inorg. Chem.*, 2012, **51**, 1111.
- 19 L. Martin, S. S. Turner, P. Day, F. E. Mabbs and E. J. L. McInnes, *J. Chem. Soc., Chem. Commun.*, 1997, 1367; L. Martin, S. S. Turner, P. Day, K. M. A. Malik, S. J. Coles and M. B. Hursthouse, *J. Chem. Soc., Chem. Commun.*, 1999, 513; L. Martin, S. S. Turner and P. Day, *Synth. Met.*, 1999, **102**, 1638.
- 20 L. Martin, P. Day, H. Akutsu, J.-i. Yamada, S.-i. Nakatsuji, W. Clegg, R. W. Harrington, P. N. Horton, M. B. Hursthouse, P. McMillan and S. Firth, *CrystEngComm*, 2007, **10**, 865.
- 21 L. Martin, P. Day, S.-i. Nakatsuji, J.-i. Yamada, H. Akutsu and P. Horton, *CrystEngComm*, 2010, **12**, 1369; L. Martin, S.-i. Nakatsuji, J.-i. Yamada, H. Akutsu and P. Day, *J. Mater. Chem.*, 2010, **20**, 2738–2742; L. Martin, H. Akutsu, P. N. Horton, M. B. Hursthouse, R. W. Harrington and W. Clegg, *Eur. J. Inorg. Chem.*, 2015, **11**, 1865; L. Martin, H. Akutsu, P. N. Horton and M. B. Hursthouse, *CrystEngComm*, 2015, **17**, 2783.
- 22 P. Guionneau, C. J. Kepert, D. Chasseau, M. R. Truter and P. Day, *Synth. Met.*, 1997, **86**, 1973.
- 23 T. Mori, A. Kobayashi, Y. Sasaki, H. Kobayashi, G. Saito and H. Inokuchi, *Bull. Chem. Soc. Jpn.*, 1984, **57**, 627. (See also <http://www.op.titech.ac.jp/lab/mori/lib/program.html>).
- 24 T. G. Prokhorova, S. S. Khasanov, L. V. Zorina, L. I. Buravov, V. A. Tkacheva, A. A. Baskakov, R. B. Morgunov, M. Gener, E. Canadell, R. P. Shibaeva and E. B. Yagubskii, *Adv. Funct. Mater.*, 2003, **13**, 403.
- 25 S. Rashid, S. S. Turner, D. LePevelen, P. Day, M. E. Light, M. B. Hursthouse, S. Firth and R. J. H. Clark, *Inorg. Chem.*, 2001, **40**, 5304.
- 26 H. Seo, *J. Phys. Soc. Jpn.*, 2000, **69**, 805.
- 27 M. E. Lines, *J. Chem. Phys. Solids*, 1970, **31**, 101.
- 28 R. Arita, Y. Sugawa, K. Kuroki and H. Aoki, *Phys. Rev. Lett.*, 2002, **88**, 127202; A. Mielke and H. Tasaki, *Commun. Math. Phys.*, 1993, **158**, 341.
- 29 K. Mori, H. Usui, H. Sakakibara and K. Kuroki, *AIP Adv.*, 2012, **2**, 042108.
- 30 N. Senda, *Idemitsu Tech. Rep.*, 2006, **49**, 106.
- 31 M. Suda, N. Kameyama, A. Ikegami and Y. Einaga, *J. Am. Chem. Soc.*, 2009, **131**, 865.
- 32 R. Gausepohl, P. Buskens, J. Kleinen, A. Bruckmann, C. W. Lehmann, J. Klankermayer and W. Leitner, *Angew. Chem., Int. Ed.*, 2006, **45**, 3689.

